

Evaluation of Boltzmann's H-function for Particles with Orientational Degrees of Freedom

Shubham Kumar and Biman Bagchi*

Solid State and Structural Chemistry Unit, Indian Institute of Science,
Bengaluru-560012, Karnataka, India

*Email: profbiman@gmail.com; bbagchi@iisc.ac.in

Abstract

Boltzmann's H-function $H(t)$ holds a venerable place in the history of science. However, it seems never to have been evaluated for particles with orientational degrees of freedom. We generalize Boltzmann's H-function to a gas of molecules that can both rotate and translate and on collision exchange both momentum and angular momentum, obeying conservation laws. We evaluate the time (t) evolution of single-particle joint probability distribution $f^{(1)}(\mathbf{p}, \mathbf{L}, t)$ for linear (\mathbf{p}) and angular (\mathbf{L}) momenta from an initial nonequilibrium state by molecular dynamics simulations. We consider both prolate and oblate-shaped particles, interacting by well-known Gay-Berne potential that depends both on position \mathbf{r} and orientation ($\mathbf{\Omega}$) vectors. We calculate the relaxation of the generalized *molecular* $H(t)$ from several initial ($t=0$) nonequilibrium states. In the long-time limit, the H function saturates to its exact equilibrium value, which is the sum of translational and rotational contributions to the respective entropies. Both the translational and rotational components of $H(t)$ decay nearly exponentially with time; the rotational component is more sensitive to the molecular shape that enters through the aspect ratio. A remarkable rapid decrease in the rotational relaxation time is observed as the spherical limit is approached, in a way tantalizingly reminiscent of Hu-Zwanzig hydrodynamic prediction with slip boundary condition. Additionally, we obtain $H(t)$ analytically by solving the appropriate translational and rotational Fokker-Planck equation and obtain a modest agreement with simulations. We observe a remarkable signature of translation-rotation coupling as a function of molecular shape, captured through a physically meaningful differential term that quantifies the magnitude of translation-rotation coupling.

I. INTRODUCTION

In 1872, Ludwig Boltzmann introduced his H-function and H-theorem. The latter is one of the most celebrated theorems of physical science. It paved the way for the development of nonequilibrium statistical mechanics. [1–6] Boltzmann was the first to attempt to establish a relation between relaxation and entropy. Even after 150 years, Boltzmann’s H-function continues to play an important role in the study of nonequilibrium relaxation phenomena, partly because of its close relationship with entropy. [3–8] Boltzmann’s function continues to find wide use today, often with suitable generalization, as introduced by Kubo and employed by many. [8–10] *H(t), in various forms, is widely regarded as a function to describe the time dependence of entropy in a nonequilibrium process.*

Boltzmann’s H-function $H(t)$, in its original form, is defined by the following d -dimensional integration [1–8]

$$H(t) = - \int d\mathbf{p} f^{(1)}(\mathbf{p}, t) \ln f^{(1)}(\mathbf{p}, t). \quad (1)$$

Here, \mathbf{p} is the linear momentum of the particle, defined as $\mathbf{p} = m\mathbf{v}$; m is the mass of the particle and \mathbf{v} is the velocity of the particle. $f^{(1)}(\mathbf{p}, t)$ is the time-dependent singlet linear momentum distribution function. Note that Boltzmann considered only translational degrees of freedom in three dimensions and considered only spherical atoms. *We are not aware of any studies that included rotational degrees of freedom in the generalization considered here.* The constraint to spheres has remained a limitation because the rotational degree of freedom could play an important, even dominant, role in many relaxation processes.

Boltzmann’s H theorem states that $H(t)$ is an ever-increasing function of time till it reaches the equilibrium value, which is essentially the same as the entropy for a dilute gas. [1–8] The H-Theorem is stated as

$$\frac{dH}{dt} \geq 0. \quad (2)$$

Here, the equality sign is satisfied only at equilibrium when the distribution takes on the Maxwell form. That is, if $f^{(1)}(\mathbf{p}, t)$ is not an equilibrium distribution, the H-function will increase until the equilibrium distribution is obtained.

However, most of the discussions of Boltzmann's H-theorem and H-function center around the Boltzmann kinetic equation (also known as the Boltzmann transport equation), which is strictly applicable only to a dilute gas of atoms. [7] The form of the H-theorem evolves from the necessity to demonstrate that the assumption of molecular chaos does not disrupt the progress to the correct equilibrium distribution over a long time. As it is well-known, Boltzmann's kinetic equation has been used in various areas, from astrophysics to hydrodynamics to chemical kinetics, and remains a venerable subject of classroom studies and academic discussions, not just in research. However, despite the importance, we find limited, precise numerical (or, analytical) calculations of the evolution of Boltzmann's H-function from a well-defined nonequilibrium state. [7,9–14] And, all the available calculations are restricted to atoms with no orientational degrees of freedom. This has long remained a lacuna in the area of time-dependent statistical mechanics. In fact, we are not aware of any analytical form of $H(t)$. The latter lacuna has recently been removed in Ref. [15] where we carried out a detailed numerical evaluation of $H(t)$ for a system of particles interacting via (i) hard sphere, (ii) soft sphere, and (iii) Lennard-Jones potentials. [15] We created different nonequilibrium states and studied the time evolution of the H-function in one, two, and three dimensions by calculating $f^{(1)}(\mathbf{p}, t)$ itself. It was observed that Boltzmann's function captured many of the nuances of the relaxation phenomena. For example, in the one-dimensional Lennard-Jones system, it captured a correlated motion with a long lifespan, originating from single file motion. Another interesting result was a clear demonstration of the linear response of the system to initial perturbation even when the distribution function at intermediate times appeared quite different.

All the reported theoretical and computer simulation studies of $H(t)$ employed spherical atoms/molecules with radially symmetric potentials, although real molecular systems are almost always non-spherical, and many experimental results pertain to rotational dynamics. This extra channel needs attention as non-spherical molecules can rotate to facilitate molecular motion. [16]

The organization of the rest of the paper is as follows. In Section II, we present the generalized form of Boltzmann's H-function (Eq. 3). Section III contains the simulation and the system details. Here we describe the construction of the initial nonequilibrium state. In Section IV, we present the numerical results. Here, first of all, we discuss the time evolution of the generalized H-function for prolate and oblate shaped particles. Subsequently, we discuss the aspect ratio dependence of the relaxation time of $H(t)$. After that, we introduce a physically motivated differential term that captures the presence and the magnitude of translation-rotation coupling through a discriminant $\Delta_{T-R}(t)$. This function shows interesting dynamical behavior at intermediate times. Section V presents our analytical expression of $H(t)$. In Section VI, we present a concise discussion of the results along with concluding remarks in connection with future problems.

II. GENERALIZATION TO ORIENTATION

For particles with rotational degrees of freedom, Boltzmann's kinetic equation needs to be modified. We now need to deal with the time-dependent joint probability distribution $f^{(1)}(\mathbf{r}, \mathbf{p}, \mathbf{\Omega}, \mathbf{L}, t)$ for finding an *aspherical particle* at position \mathbf{r} with linear momentum \mathbf{p} , having an orientation $\mathbf{\Omega}$ and angular momentum \mathbf{L} (defined as $\mathbf{L} = I\boldsymbol{\omega}$; $\boldsymbol{\omega}$ is the angular velocity of the particle with the moment of inertia I). We then write Boltzmann's kinetic equation generalized to include orientation as

$$\left(\frac{\partial f}{\partial t}\right)_{coll} = \iiint d\mathbf{p}_2 d\mathbf{\Omega}_2 d\mathbf{L}_2 d\mathbf{p}'_1 d\mathbf{\Omega}'_1 d\mathbf{L}'_1 d\mathbf{p}'_2 d\mathbf{\Omega}'_2 d\mathbf{L}'_2 \delta(\mathbf{P} - \mathbf{P}') \delta(\mathbf{L}_T - \mathbf{L}'_T) \delta(E - E') \times |T_{fi}|^2 (f_{1'2'}^{(2)} - f_{12}^{(2)}), \quad (3)$$

where the collisional integral is given in terms of two-particle joint probability distribution. Here, \mathbf{P} , \mathbf{L}_T , and E denote the total linear momentum, total angular momentum, and energy before a collision, respectively; \mathbf{P}' , \mathbf{L}'_T , and E' represent the total linear momentum, total angular momentum, and the total energy after the collision. The T-matrix gives the transition probability. $f^{(2)}$ is the two-body joint probability distribution function. The expression contains the conservation of energy, linear momenta, and angular momenta.

As was experienced by Evans and coworkers, [17,18] the inclusion of the rotational degrees of freedom results in an even more complex equation than we had in the original Boltzmann kinetic equation. It is highly formidable In order to proceed further towards the appropriate H-function, we need to recognize the following things. *In deriving the binary collisional event, one assumes that the collision occurs at a small volume element at position \mathbf{r} , where only the exchange of momenta occurs without any change of position.* We proceed along the same line and assume that during collision only the angular momenta are exchanged and no change in orientation takes place. It is interesting to note that this is similar to the set of simplifying assumptions made by Gordon in the study of magnetic relaxation and is well-known as the J-diffusion model. [19] However, here one assumes that the momenta and the angular momenta change on the faster time scales. The collisional integral then reduces to a simpler form,

$$\left(\frac{\partial f}{\partial t}\right)_{coll} = \iiint d\mathbf{p}_2 d\mathbf{L}_2 d\mathbf{p}'_1 d\mathbf{L}'_1 d\mathbf{p}'_2 d\mathbf{L}'_2 \delta(\mathbf{P} - \mathbf{P}') \delta(\mathbf{L}_T - \mathbf{L}'_T) \delta(E - E') \times |T_{fi}|^2 (f_{1'2'}^{(2)} - f_{12}^{(2)}). \quad (4)$$

This expression is tractable in the same way as Boltzman's original kinetic equation without orientation. In the next step, one employs the assumption of molecular chaos to

decompose the two-particle joint probability distribution $f^{(2)}(\mathbf{p}_1, \mathbf{p}_2, \mathbf{L}_1, \mathbf{L}_2, t)$ into the product of two single-particle distribution functions $f^{(1)}(\mathbf{p}, \mathbf{L}, t)$. In the subsequent steps, one needs to assure that such an approximate distribution function indeed attains the Maxwell velocity distribution in a long time. The steps are the same as documented in textbooks. [6,7] This necessitates the introduction of Boltzmann's H-function, now generalized to include the contribution of angular momentum (\mathbf{L}). The new or total Boltzmann's H-function $H_{Tot}(t)$ one obtains is given by

$$H_{Tot}(t) = - \int d\mathbf{p} d\mathbf{L} f^{(1)}(\mathbf{p}, \mathbf{L}, t) \ln f^{(1)}(\mathbf{p}, \mathbf{L}, t), \quad (5)$$

We note that the joint probability distribution may not be decomposed into a product of independent translational and rotational distribution functions.

However, even for non-spherical particles, it is still useful to define translational and angular H-functions. The translational part has already been defined by Eq. (1). The rotational part is defined in the same fashion as

$$H_{Rot}(t) = - \int d\mathbf{L} f^{(1)}(\mathbf{L}, t) \ln f^{(1)}(\mathbf{L}, t). \quad (6)$$

The intermolecular potential inherently involves translation-rotation coupling, making it impossible to decompose the joint probability distribution into the product of two independent functions. This is an important point. Because of the exchange of momentum and kinetic energy between the translational and rotational degrees of freedom, such a decomposition can lead to serious error, as indeed demonstrated in this work.

This result, in fact, reminds one of the assumptions of molecular chaos all over again, but in a different context, at the level of the single-particle joint probability distribution, while the original molecular chaos assumption involves the decomposition of two-particle distribution into the product of two one-particle distribution functions. In a long time, that is, the equilibrium limit, the translational, and the rotational momenta are decoupled, and the

function gives the total kinetic entropy of the gas. During the evolution of an initial nonequilibrium distribution function, $f^{(1)}(\mathbf{r}, \mathbf{p}, \mathbf{\Omega}, \mathbf{L}, t=0)$, it is non-trivial to obtain the time-dependent joint probability distribution $f^{(1)}(\mathbf{r}, \mathbf{p}, \mathbf{\Omega}, \mathbf{L}, t)$.

In fact, theoretically, one can construct a generalized Boltzmann's kinetic equation with arbitrary internal degrees of freedom and follow the same steps as followed by Boltzmann to arrive at Eq. (5) for the H-function. Such a definition must follow all the necessary conditions (like conservation laws and transition probabilities between states) and can serve the same purpose. In fact, Kubo *et al.* introduced an H-function involving a generalized coordinate-dependent density function but did not address any orientation-dependent function. [8]

To understand the time evolution of our generalized H-function and the validity of the H-theorem, we examine two model systems with rotational degrees of freedom. The time evolution of the generalized H-function is evaluated for symmetrical ellipsoids (ellipsoids of revolution). To be more specific, we consider a system of gas consisting of prolates and oblates and vary the aspect ratio from markedly non-spherical to spherical limits. The simulation results have been compared with analytical forms that we derive by solving the Fokker-Planck equation of motion for $f^{(1)}(\mathbf{p}, \mathbf{L}, t)$ and using the resulting expression to obtain the $H(t)$.

Our studies reveal several interesting new results. We find that the normalized rotational and translational $H(t)$ grows with similar time scales from the initial nonequilibrium state. However, their aspect ratio dependencies are strikingly different. In the following section, we describe the simulation details.

III. SIMULATION DETAILS

We have performed extensive nonequilibrium molecular dynamic simulations of dilute gases with orientational degrees of freedom (ODOF) to study the evolution of the generalized H-function, defined by Eq. (5). Our model system consists of 4000 symmetrically ellipsoidal

particles, i.e., prolates (rod-shaped molecules) or oblates (disc-shaped molecules) contained in a cubic box having the usual periodic boundary condition in each case. We have carried out these simulations in the microcanonical ensemble (constant N , V , and E). In the simulations studies where the shape and orientation of the rigid body play a crucial role, the Gay-Berne (GB) pair potential provides a convenient model for interaction between two particles. [20–23] In the GB pair potential, each spheroid i is represented by the position \mathbf{r}_i of its center of mass and a unit vector \mathbf{e}_i along the principal symmetry axis (as shown in **Figure 1**). The Gay-Berne potential for the interaction between two spheroids i and j is given by the following expression [20]

$$U_{ij}^{GB}(\mathbf{r}_{ij}, \mathbf{e}_i, \mathbf{e}_j) = 4\varepsilon_{ij}(\hat{\mathbf{r}}_{ij}, \mathbf{e}_i, \mathbf{e}_j)(\rho_{ij}^{-12} - \rho_{ij}^{-6}), \quad (7)$$

where

$$\rho_{ij} = \frac{r_{ij} - \sigma(\hat{\mathbf{r}}_{ij}, \mathbf{e}_i, \mathbf{e}_j) + \sigma_0}{\sigma_0}. \quad (8)$$

Here, σ_0 defines the cross-sectional diameter along the breadth, r_{ij} is the distance between the two centers of mass, and $\hat{\mathbf{r}}_{ij} = \mathbf{r}_{ij} / r_{ij}$ is a unit vector along the intermolecular separation vector \mathbf{r}_{ij} . The molecular shape parameter $\sigma(\hat{\mathbf{r}}_{ij}, \mathbf{e}_i, \mathbf{e}_j)$ is given by

$$\sigma(\hat{\mathbf{r}}_{ij}, \mathbf{e}_i, \mathbf{e}_j) = \sigma_0 \left[1 - \frac{\chi}{2} \left\{ \frac{(\mathbf{e}_i \cdot \hat{\mathbf{r}}_{ij} + \mathbf{e}_j \cdot \hat{\mathbf{r}}_{ij})^2}{1 + \chi(\mathbf{e}_i \cdot \mathbf{e}_j)} - \frac{(\mathbf{e}_i \cdot \hat{\mathbf{r}}_{ij} - \mathbf{e}_j \cdot \hat{\mathbf{r}}_{ij})^2}{1 - \chi(\mathbf{e}_i \cdot \mathbf{e}_j)} \right\} \right]^{-1/2}, \quad (9)$$

where $\chi = \frac{(\kappa^2 - 1)}{(\kappa^2 + 1)}$. Here κ denotes the aspect ratio of the spheroid and is given by $\kappa = \sigma_E / \sigma_S$.

σ_E is the molecular length along the principal symmetry axis and $\sigma_S = \sigma_0$.

The energy parameter $\varepsilon(\hat{\mathbf{r}}_{ij}, \mathbf{e}_i, \mathbf{e}_j)$ is given by

$$\varepsilon_{ij}(\hat{\mathbf{r}}_{ij}, \mathbf{e}_i, \mathbf{e}_j) = \varepsilon_0 [\varepsilon_1(\mathbf{e}_i, \mathbf{e}_j)]^\nu [\varepsilon_2(\hat{\mathbf{r}}_{ij}, \mathbf{e}_i, \mathbf{e}_j)]^\mu, \quad (10)$$

where μ and ν are two exponents that are adjustable, and

$$\varepsilon_1(\mathbf{e}_i, \mathbf{e}_j) = \left[1 - \chi^2 (\mathbf{e}_i \cdot \mathbf{e}_j)^2 \right]^{-1/2}, \quad (11)$$

and

$$\varepsilon_2(\hat{\mathbf{r}}_{ij}, \mathbf{e}_i, \mathbf{e}_j) = 1 - \frac{\chi'}{2} \left[\frac{(\mathbf{e}_i \cdot \hat{\mathbf{r}}_{ij} + \mathbf{e}_j \cdot \hat{\mathbf{r}}_{ij})^2}{1 + \chi'(\mathbf{e}_i \cdot \mathbf{e}_j)} + \frac{(\mathbf{e}_i \cdot \hat{\mathbf{r}}_{ij} - \mathbf{e}_j \cdot \hat{\mathbf{r}}_{ij})^2}{1 - \chi'(\mathbf{e}_i \cdot \mathbf{e}_j)} \right]. \quad (12)$$

Here, $\chi' = (\kappa'^{1/\mu} - 1) / (\kappa'^{1/\mu} + 1)$ with $\kappa' = \varepsilon_S / \varepsilon_E$. ε_S represents the depth of the minimum of the potential for a pair of ellipsoids when they are aligned side-by-side [$\varepsilon_S = \varepsilon_0$], and ε_E is the corresponding depth for end-to-end alignment. The functional form of the Gay-Berne potential and a schematic diagram of a pair of ellipsoids interacting via the Gay-Berne potential is shown in **Figure 1**.

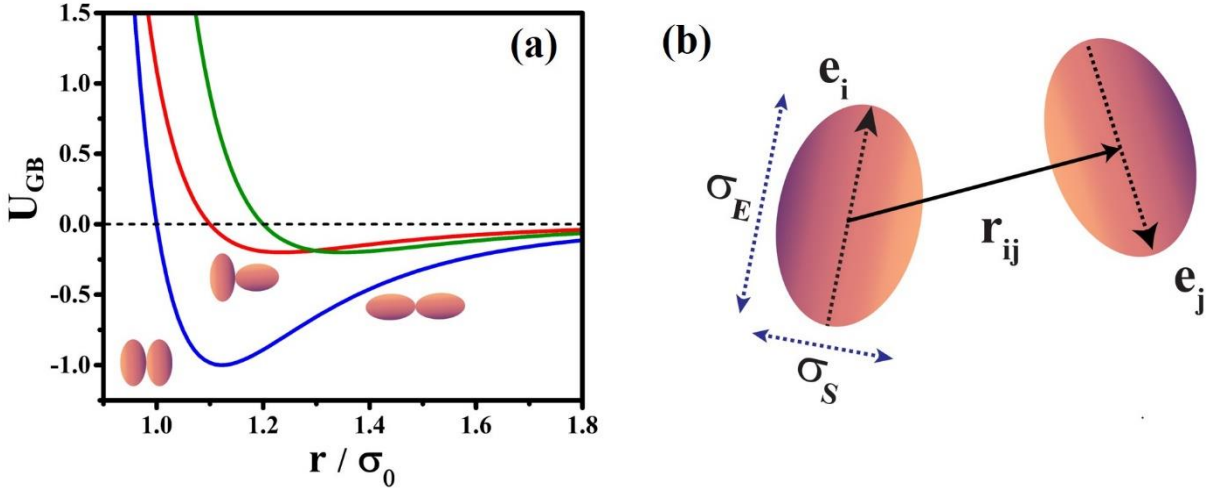


Figure 1. (a) Functional form of the Gay-Berne potential characterized by a set of parameters (κ , 5, 2, 1). The ratio of the energy depth of the side-by-side configuration (corresponding to the deepest energy depth, blue line) to that of the end-to-end configuration (corresponding to the shallowest energy depth, green line) shows the value of $\kappa' = 5.0$. (b) Schematic diagram of a pair of ellipsoids defined by the Gay-Berne potential parameter.

All quantities are given here in reduced units, defined in terms of the GB potential parameters σ_0 and ε_0 : length in the units of σ_0 , time in the units of $(\sigma_0^2 m / \varepsilon_0)^{1/2}$, m being the mass of the spheroid, and temperature in units of ε_0 / k_B , k_B being the Boltzmann constant. ε_0 has been taken to unity. We have set the mass (m) of the ellipsoids equal to unity i.e., $m = 1.0$. The inertia tensor is chosen as $I_x = I_y$. The value of the I_z component is irrelevant due to the conservation of the angular velocity along the symmetry (z) axis of the ellipsoid. [24]

The reduced density $\left(\rho^* = \frac{N \times m}{V} \times \frac{4\pi\sigma_s^2\sigma_e}{3m} \right)$ is taken as 0.10 for all the systems, where N is the total number of particles, and V is the volume of the simulation box.

The Gay-Berne potential defines a family of potential, each member of which is characterized by a set of four parameters $(\kappa, \kappa', \mu \text{ and } \nu)$. κ being the aspect ratio, provides a measure of the shape anisotropy while κ' provides a measure of the anisotropy of the well depth, which can also be controlled by the two parameters μ and ν . In our study, the spheroid is characterized by these parameters as $(\kappa, 5, 2 \text{ and } 1)$. The aspect ratio (κ) for prolates is varied from 1.05 to 3.0, whereas, for oblates, it is varied from 0.98 to 0.40.

The initial configurations (position) were taken from equilibrium simulations in the canonical (NVT) ensemble corresponding to $T^* = 2.0$. Thereafter, the initial nonequilibrium state is created by taking the amplitude of both linear and angular velocities of all the particles exactly the same; the magnitude is in accordance with the equipartition theorem corresponding to the reduced temperature $T^* = k_B T / \varepsilon_0 = 2.0$. This approach assures that the total energy remains constant.

The equations of motion have been integrated following the velocity-Verlet algorithm [25,26] with the integration time step of $\delta t^* = 0.001 \tau$. Here τ represents the scaled

time, defined as $\tau = \sigma_0 \sqrt{m/\varepsilon_0}$. In this work, we have converted the time scales from reduced time (t^*) to real-time (t) using relation $t^* = t \sqrt{\frac{\varepsilon_0}{m\sigma_0^2}}$, where the values of ε_0 , m and σ_0 have been taken corresponding to that of argon atom i.e., $\varepsilon_0 / k_B = 119.8 \text{ K}$, $m = 0.03994 \text{ kg / mol}$ and $\sigma_0 = 3.405 \times 10^{-10} \text{ m}$. We ran five independent simulations in order to achieve the converged results, and the outcomes were averaged over all of these runs.

IV. RESULTS AND DISCUSSION

We study the time evolution of the generalized (or total) H-function, defined by Eq. (5), using a series of nonequilibrium molecular dynamics simulations of dilute gases with orientational degrees of freedom (ODOF) interacting via the Gay-Berne pair potential. In the following subsections, we present the numerical results obtained from our simulations and compare them with theoretical closed-form expressions derived from the Fokker-Planck equations.

(A) Time dependence of H-function

In **Figures 2 (a) and 2 (b)**, we show the time evolution of the generalized (or total) Boltzmann H-function $H_{Tot}(t)$, as well as its translational and rotational components for oblate ($\kappa = 0.8$) and prolate ($\kappa = 2.0$), respectively, at reduced density, $\rho^* = 0.10$ and average reduced temperature, $T^* = 2.0$, which is obtained by a procedure mentioned in the Methods sections. We observe that for both oblates and prolates, the generalized Boltzmann H-function, as well as its translational and rotational components, sharply increase in a short time, followed by a subsequently monotonous approach to the equilibrium value (shown by dotted lines) at a longer time, which is the equilibrium value at the chosen temperature. Further, we find that, in

the long-time limit, the generalized Boltzmann H-function $H_{Tot}(t)$ saturates to the equilibrium value, which is the sum of translational and rotational contributions. However, at intermediate times, the sum of translational and rotational contributions is not equivalent to the generalized Boltzmann H-function $H_{Tot}(t)$. *It can be attributed to the translational-rotational coupling in the ellipsoids.* That is, the time-dependent joint probability distribution is not decomposable into the product of two terms, as is possible under equilibrium conditions.

To get the relaxation times of the generalized Boltzmann H-function and its translational and rotational parts, the respective H-functions have been fitted with the functional form $H(t) = H_{eq} + \left[(H(0) - H_{eq}) \exp(-t / \tau) \right]$. In **Figures 2 (c) and 2 (d)**, we show normalized $H(t)$, defined as $\left((H(t) - H_{eq}) / (H(0) - H_{eq}) \right)$ and its exponential fit for oblate ($\kappa = 0.8$) and prolate ($\kappa = 2.0$), respectively. The relaxation times (τ) for the generalized, translational, and rotational H-functions are given in **Table 1**. We observe that the relaxation time of the generalized H-function lies in between the relaxation times of the translational and rotational components.

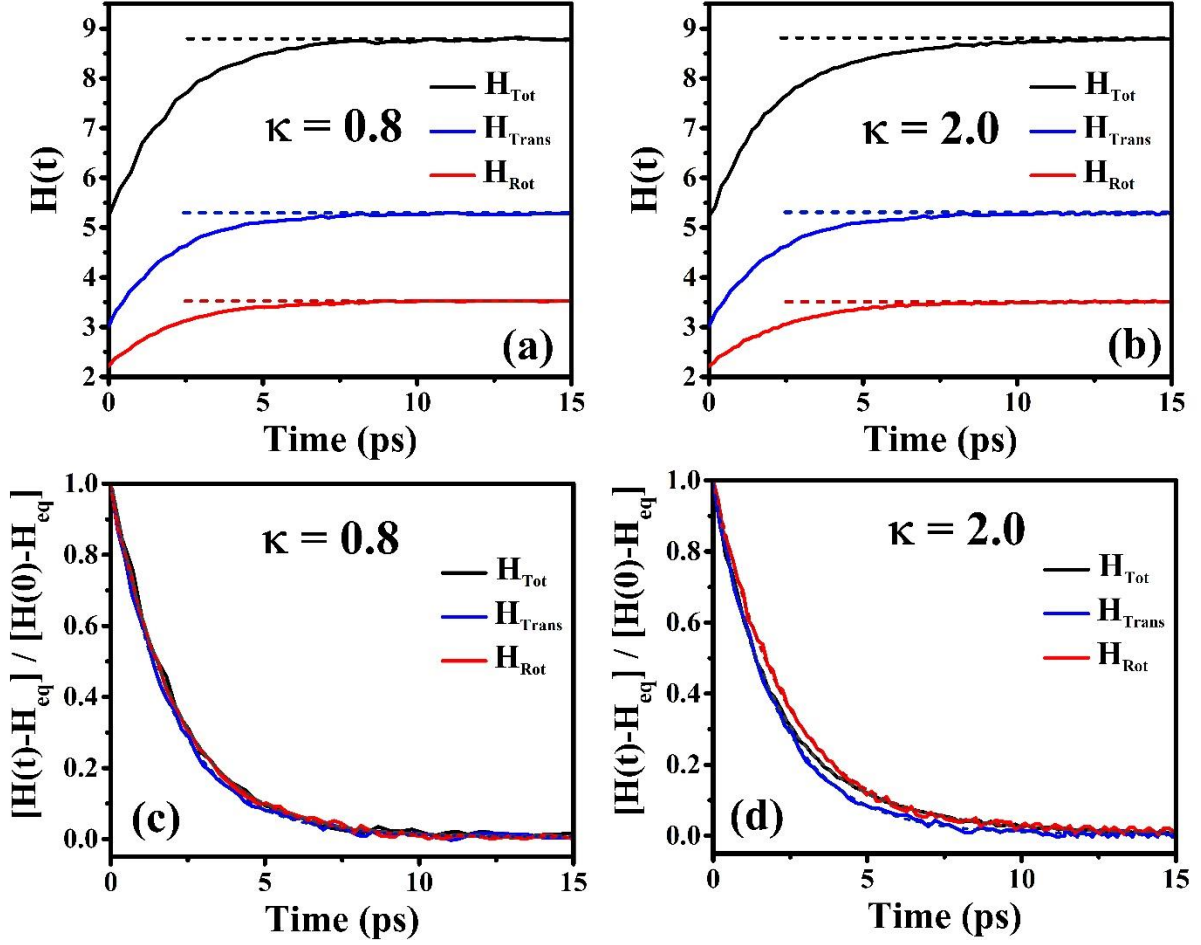


Figure 2. Time evolution of the generalized, translational, and rotational H-functions obtained via computer simulations for (a) oblate ($\kappa = 0.8$) and (b) prolate ($\kappa = 2.0$) systems of dilute gases (at reduced density $\rho^* = 0.10$, and average reduced temperature, $T^* = 2.0$) interacting with Gay-Berne potential. In all the cases, the H-function increases monotonically and then attains equilibrium at a longer time, which is the equilibrium value at the final temperature, shown by corresponding dashed lines in the figures. Panels (c) and (d) depict the time evolution of the normalized H(t) [for the results shown in (a) and (b), respectively]. The corresponding dotted lines show the exponential fitting of the normalized H(t).

An important point to note here is that the rotational contribution to the final equilibrium value of $H(t)$ is about half of that of the translational value. This is a significant observation because even in the case of water molecules in the liquid phase, the rotational contribution is significant but smaller by a similar proportion than the translational component. [27] In view of the present observation, it would be interesting to calculate the H-function for real molecules like water, carbon dioxide, and so forth.

Table 1. The relaxation times obtained by the exponential fitting of the generalized, translational, and rotational H-functions for oblate ($\kappa = 0.8$) and prolate ($\kappa = 2.0$).

| System | Relaxation Time (in ps) | | |
|--|-------------------------|----------------|--------------|
| | τ_{Tot} | τ_{Trans} | τ_{Rot} |
| Oblate ($\kappa = 0.8$) | 2.08 | 1.96 | 2.12 |
| Prolate ($\kappa = 2.0$) | 2.14 | 1.99 | 2.34 |

(B) Aspect ratio dependence

In order to get an insight into the effect of the aspect ratio of ellipsoids on the relaxation times of the H-function, we have computed the H-functions for different aspect ratios of oblates and prolates. In **Figure 3 (a)**, we show the variation in the relaxation time of the generalized Boltzmann H -function $H_{Tot}(t)$ as a function of the aspect ratio of ellipsoids. The variation of the relaxation times of translational and rotational H-functions with the aspect ratio of ellipsoids is shown in **Figure 3 (b)**. It is evident from **Figure 3** that the nonequilibrium relaxation function $H(t)$ is sensitive to the aspect ratio of the ellipsoids. The relaxation time gets slower as the particle becomes either more disc-like or rod-like. Further, we observe that the rotational relaxation is more sensitive to the aspect ratio as compared to the translational relaxation time.

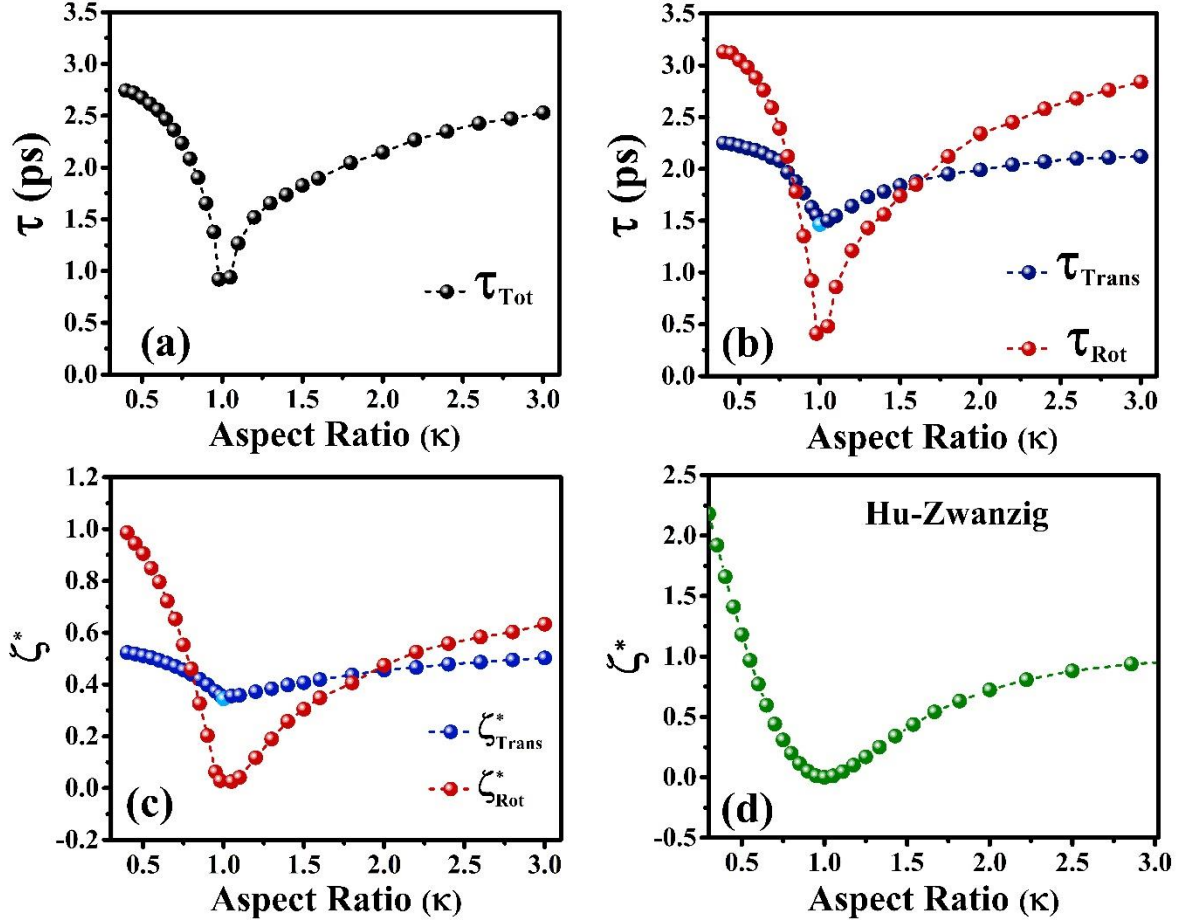


Figure 3. The variation of the relaxation time obtained by the exponential fit of (a) generalized and (b) translational and rotational H-functions with the aspect ratio of the ellipsoids. It is to be noted that the rotational relaxation is more sensitive to the aspect ratio. At $\kappa = 1$, the relaxation time of the translational H-function corresponds to the spherical particles interacting via Lennard-Jones potential (shown by the sky-blue symbol). (c) The variation of the translational (ζ_{Trans}) and rotational (ζ_{Rot}) frictions with the aspect ratio of the ellipsoids. As the spherical limit is approached, a rapid decrease in the rotational friction is observed, which is consistent with the hydrodynamic predictions of Hu and Zwanzig (panel (d)) with slip boundary condition [J. Chem. Phys. 4354, (1974)].

To understand the strong aspect ratio dependence of the relaxation times, we have calculated the linear and angular velocity time-correlation functions as well as the corresponding frictions. **Figures 4(a) to 4(c)** depict the normalized linear and angular velocity time-correlation functions of oblates with different aspect ratios ($\kappa = 0.95, 0.80$ and 0.65). The

time evolution of the normalized linear and angular velocity time-correlation functions of prolates with three different aspect ratios ($\kappa=1.2, 2.0$ and 2.4) are shown in **Figures 4(d) to 4(f)**. It is observed that when the aspect ratio of the ellipsoid is close to one, the decay of the angular velocity autocorrelation function is slower than that of the linear velocity autocorrelation function. However, the decay of the angular velocity autocorrelation function becomes faster as the particle becomes either more disc-like or rod-like. This behavior is likely to originate from the fact that in extreme limits, collisions are more likely to randomize the velocities. This aspect deserves further study.

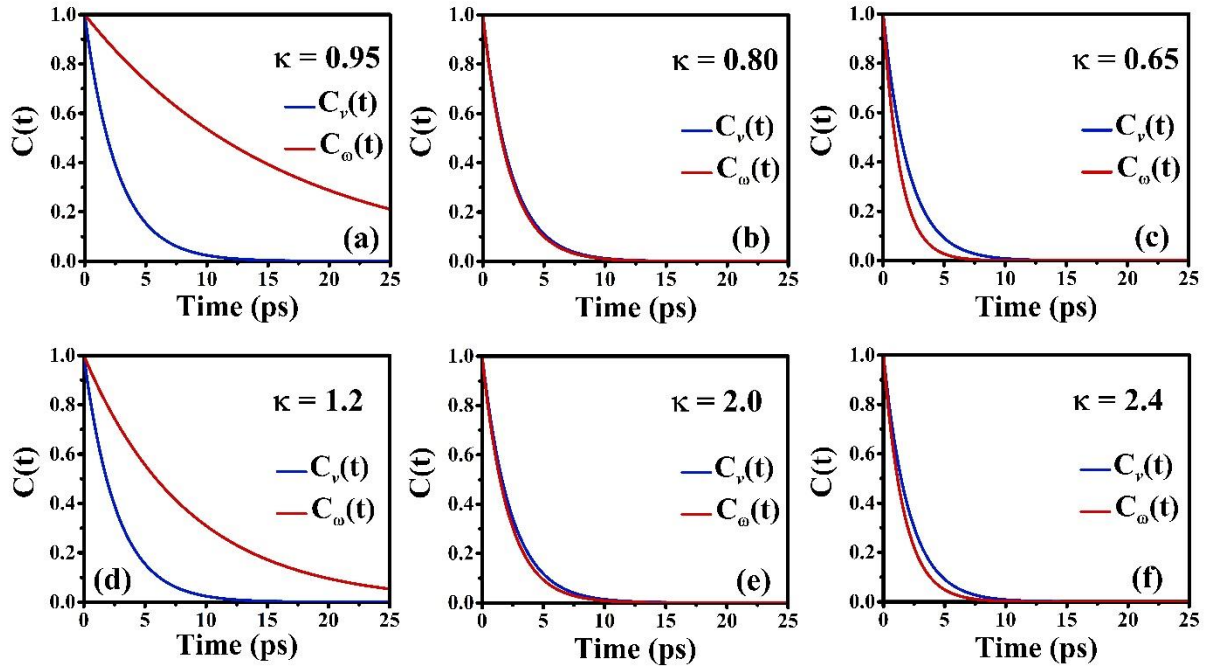


Figure 4. The normalized linear and angular velocity autocorrelation functions of oblates when (a) $\kappa = 0.95$, (b) $\kappa = 0.80$, (c) $\kappa = 0.65$, and for prolates when (d) $\kappa = 1.2$, (e) $\kappa = 2.0$, and (f) $\kappa = 2.4$, respectively. It is to be noted that the decay of the angular velocity autocorrelation function becomes faster as the particle becomes either more disc-like or rod-like.

We have calculated the translational friction (ζ_{Trans}) via the integration of the linear velocity time-correlation function and using Einstein's relation $D_{Trans} = k_B T / \zeta_{Trans}$. Similarly,

the rotational friction (ζ_{Rot}) is obtained via the angular velocity time-correlation function using Einstein's relation $D_{Rot} = k_B T / \zeta_{Rot}$. [28,29]

In **Figure 3(c)**, we show the variation of the translational and rotational friction of ellipsoids as a function of the aspect ratio. We find that the rotational friction (ζ_{Rot}) shows strong aspect ratio dependence as observed for the relaxation times of rotational H-function. It is to be noted that the variation of the rotational friction with the aspect ratio behaves in a similar manner to that predicted by the hydrodynamic theory of Hu and Zwanzig (as shown in **Figure 3(d)**), who obtained the friction for prolate and oblate ellipsoids under the slip boundary condition. [30] Such a dramatic behavior is not predicted for rotational friction under the stick boundary condition because the rotational friction itself is very large for sticky spheres.

(C) Translation-rotation coupling

In order to understand the similarity between the aspect-ratio dependence of the translational and rotational relaxation times, we study translation-rotation coupling. To quantify the coupling between the translational and rotational motion of ellipsoids evolving from initial nonequilibrium condition, we define a quantity $\Delta_{T-R}(t)$ in the following manner

$$\Delta_{T-R}(t) = \int d\mathbf{p} d\mathbf{L} [f(\mathbf{p}, \mathbf{L}, t) - f(\mathbf{p}, t) f(\mathbf{L}, t)]. \quad (13)$$

Here, the symbols have their usual meaning, as described earlier.

In **Figure 5**, we show the variation of the quantity $\Delta_{T-R}(t)$ as a function of time for oblate ($\kappa = 0.8$) and prolate ($\kappa = 2.0$) when the system is evolving from the initial nonequilibrium state to the equilibrium state. At $t = 0$, the quantity $\Delta_{T-R}(t)$ is zero since the initial nonequilibrium state is chosen such that there is no coupling between the translational and rotational motion of the particles. However, at intermediate time steps, we find that

$\Delta_{T-R}(t)$ acquires a non-zero value suggesting a significant coupling between the translational and rotational motion of the ellipsoids. Further, as the system approaches the equilibrium, $\Delta_{T-R}(t)$ becomes zero due to the decoupling between translational and rotational dynamics. It is to be noted that the function $\Delta_{T-R}(t)$ is dependent on the initial nonequilibrium conditions.

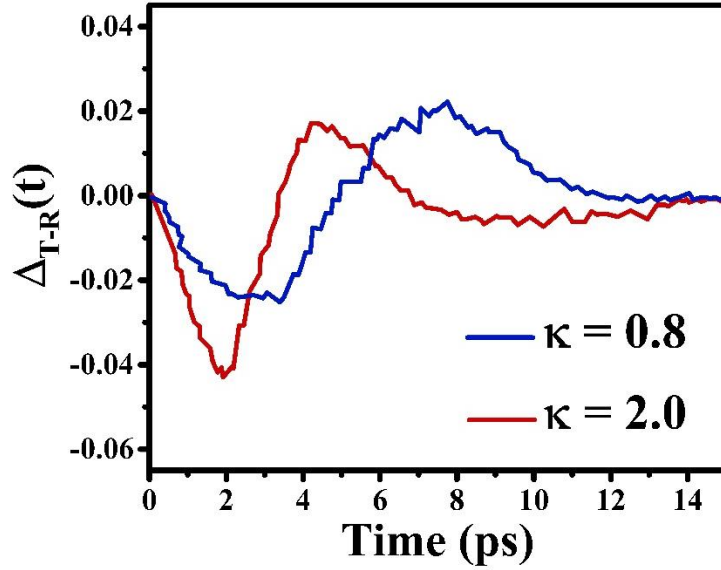


Figure 5. A measure of translation-rotation coupling. Time evolution of $\Delta_{T-R}(t)$ for oblate ($\kappa = 0.8$) and prolate ($\kappa = 2.0$), when the system is evolving from a nonequilibrium state to the equilibrium state. At $t=0$, $\Delta_{T-R}(t)$ is zero as the initial state is chosen such that there is no coupling between the translational and rotational motion of the particles. At intermediate times, it acquires a non-zero value due to translational-rotational coupling and again becomes zero in the long-time limit due to decoupling.

(D) Moment of inertia dependence

In the earlier sections, we have discussed the aspect ratio dependence of translational, rotational, and generalized $H(t)$, keeping the moment of inertia fixed. The next obvious question arises what would be the relaxation time of $H(t)$ if the moment of inertia of spheroids is varied, keeping the aspect ratio fixed. To examine this, we have obtained the time evolution

of translational, rotational, and generalized $H(t)$ corresponding to different moments of inertia of ellipsoids for two different fixed aspect ratios.

In **Figures 6(a)** and **6(b)**, we show the variation in the relaxation time of the translational, rotational, and generalized H -functions as a function of the moment of inertia of oblate ($\kappa = 0.8$) and prolate ($\kappa = 2.0$), respectively. We observe that the relaxation time of the rotational H -function shows a strong dependence on the moment of inertia of ellipsoids for both prolates and oblates. As the moment of inertia increases, the relaxation of the rotational H -function becomes slower. Further, the relatively weak dependence of the translational relaxation time on the moment of inertia of ellipsoids can be attributed to translational-rotational coupling. As observed in earlier cases, the relaxation time of the generalized (or total) H -function lies in between that of the rotational and translation H -functions.

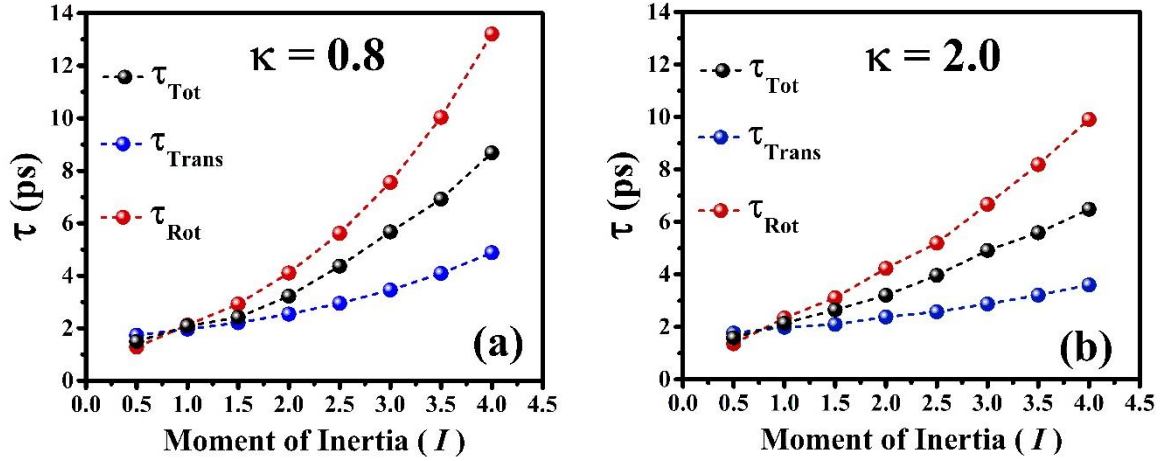


Figure 6. The variation of the relaxation time obtained by the exponential fit of generalized, translational, and rotational $H(t)$ as a function of the moment of inertia of (a) oblate ($\kappa = 0.8$) and (b) prolate ($\kappa = 2.0$), for systems of dilute gases (at reduced density $\rho^* = 0.10$, and average reduced temperature, $T^* = 2.0$). It is to be noted that as the moment of inertia increases, the relaxation of $H(t)$ becomes slower.

V. ANALYTICAL EXPRESSION OF H(t)

A closed-form analytical expression for the H-function can be derived by using the solution of the Fokker-Planck equation of the single-particle momentum distribution. [15] The Fokker-Planck equation in the linear momentum space for $f^{(1)}(\mathbf{p}, t)$ is given by [8,29]

$$\frac{\partial \delta f^{(1)}(\mathbf{p}, t)}{\partial t} = \zeta_{Trans} \left(\frac{\partial}{\partial \mathbf{p}} \left[\frac{\mathbf{p}}{m} + \langle E \rangle \frac{\partial}{\partial \mathbf{p}} \right] \right) \delta f(\mathbf{p}, t) \quad (14)$$

where $\langle E \rangle$ is the average energy, $\partial / \partial \mathbf{p}$ is the D-dimensional gradient in linear momentum space. In three-dimension, the above equation has the solution,

$$f^{(1)}(\mathbf{p}, t) = \frac{1}{(2\pi m k_B T (1 - \Gamma^2(t)))^{3/2}} \exp(-[\mathbf{p} - \mathbf{p}_0 \Gamma(t)]^2 / (2m k_B T (1 - \Gamma^2(t)))) \quad (15)$$

where, $\Gamma(t) = e^{-\zeta_{Trans} t}$, ζ_{Trans} being the translational friction of the system. By putting equation (7) into equation (1), followed by some algebraic manipulations, one can obtain a closed-form analytic expression for translational H-function as follows, [15]

$$H_{Trans}(t) = -\frac{3}{2} \ln \left(\frac{1}{2\pi m k_B T (1 - \exp(-2\zeta_{Trans} t))} \right) + \frac{3}{2}. \quad (16)$$

The above elegant expression of the translational H-function needs the input of the translational friction.

Analogous to the closed-form analytical expression for the translational H-function, one can obtain an analytical expression for the rotational H-function using the Fokker-Planck equation for rotational motion. The closed-form analytical expression of rotational H-function for symmetrical ellipsoids is given by,

$$H_{Rot}(t) = -\ln \left(\frac{1}{2\pi I k_B T (1 - \exp(-2\zeta_{Rot} t))} \right) + 1 \quad (17)$$

The above expression of the rotational H-function needs the input of the rotational friction

$$\zeta_{\text{Rot}}.$$

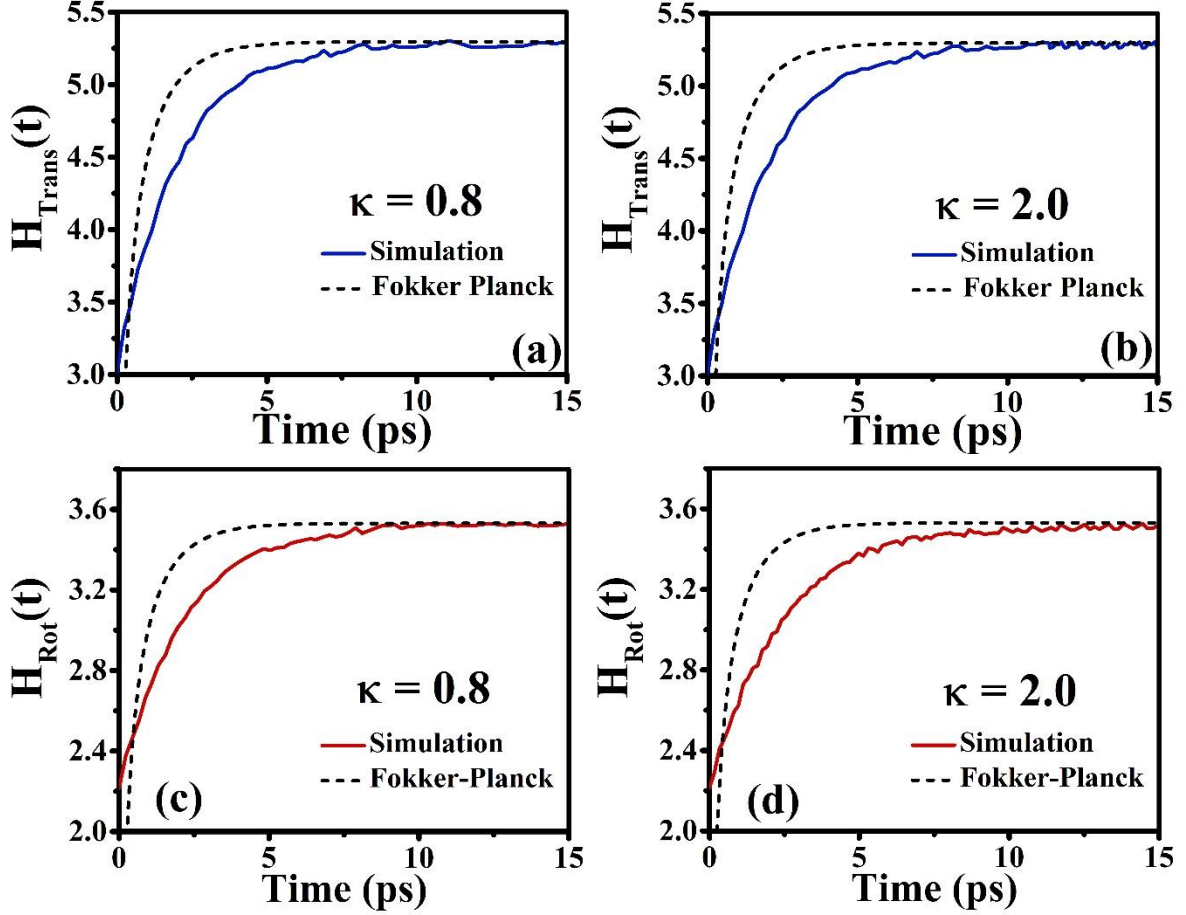


Figure 7. The comparison of translational H-function obtained via computer simulation with the analytical solution from the Fokker-Planck equation given by equation (14) for (a) oblate ($\kappa = 0.8$) and (b) prolate ($\kappa = 2.0$). Panels (c) and (d) depict the comparison of rotational H-function obtained via simulation with the analytical solution from the Fokker-Planck equation given by equation (15) for oblate ($\kappa = 0.8$) and prolate ($\kappa = 2.0$), respectively.

In **Figure 7**, we compare the results obtained via simulation and the closed-form analytical expressions of translation and rotational H-function for oblate ($\kappa = 0.8$) and prolate ($\kappa = 2.0$). There is an interesting observation to be made here. For atomic systems, the expression of $H(t)$ from the Fokker-Planck equation provides almost a quantitative agreement with the simulated values, except at a very short time. [15] The same level of agreement is not

observed in the present case. We attribute again to the presence of translation-rotation coupling, especially strong at the intermediate times.

VI. CONCLUDING REMARKS AND FUTURE PROBLEMS

Here, we provide a generalization of the famous Boltzmann H-function, $H(t)$, *to include the orientational degree of freedom*, we believe, for the first time. Most, (if not all) previous calculations considered only spherical atoms. [11,15] We evaluate the generalized $H(t)$ for an interacting system of molecules in the gas phase from an initial nonequilibrium dynamical state. The calculations of $H(t)$ reveal interesting aspects of the relaxation of the nonequilibrium distribution function, summarized below.

(i) First, the orientational relaxation is found to be more sensitive than the translational mode to the aspect ratio of the ellipsoid of revolution, although the time scales are similar.

(ii) Second, the orientational relaxation rate of $H(t)$ increases rapidly as the perfect sphere limit is approached in a manner reminiscent of the slip hydrodynamics boundary condition in rotation.

(iii) The effect of this rapid increase in orientational relaxation rate (as measured by $H(t)$) also shows up in the translational component, which is a new result, due to a coupling between translation and rotational modes, but not fully understood yet. The presence and the magnitude of translation-rotation coupling are captured through a discriminant $\Delta_{T-R}(t)$ defined by Eq. (13). This function shows interesting time dependence.

(iv) We find that a simple Fokker-Planck equation with decoupling between translation and orientation components does not provide a quantitative description of the relaxation function either for the translational or rotational component. This is entirely different from what was observed in an earlier work, where molecules interact with only radial interaction. [15] In that

case, the Fokker-Planck equation was found to provide a fairly quantitative agreement of the relaxation except at very short times.

The present study opens the door for further research. A theory is needed to understand the translation-rotation coupling, at least at the level of the Fokker-Planck equation. Although an earlier study by Deutch and Oppenheim [31] addressed this point, no numerical implementation was carried out. This remains a worthwhile project for the future. In fact, earlier studies by Chandra and Bagchi [32] considered the role of translation and rotational density contributions to the rotational and translational friction and discussed the translation-rotation coupling. However, an explicit demonstration of such coupling as demonstrated here was not available earlier.

Next, the present study can also be extended to the study of binary mixtures. In particular, the study of an ellipsoidal particle in a sea of spheres should be studied as this model was considered earlier by Evans and coworkers [17,18] and also Vasanthi *et al.* [33,34] It will be particularly interesting to study the Boltzmann function for a binary mixture of prolates and oblates.

In conclusion, we would like to stress the uniqueness of the present study in understanding the dynamics of molecular liquids, particularly in the gas phase. Evans and coworkers [17,18] earlier derived expressions for the rotational Enskog friction, which can now be used in the Fokker-Planck equation to understand translation-rotation coupling in such liquids. This is a non-trivial problem but deserves further study. The present study is expected to retain some relevance even in denser (gas or liquid) systems where potential energy contribution may dominate the total value of the entropy.

Acknowledgments: BB thanks the Science and Engineering Research Board (SERB), India, for the National Science Chair Professorship and the Department of Science and Technology, India, for partial research funding. SK thanks the Council of Scientific and Industrial Research (CSIR), India, for a research fellowship.

References

- [1] L. Boltzmann, *Weitere Studien Über Das Wärmegleichgewicht Unter Gasmolekülen*, Sitzungsberichte Akad. Der Wissenschaften **66**, 275 (1872).
- [2] L. Boltzmann, *English Translation “Further Studies on the Thermal Equilibrium of Gas Molecules,”* Hist. Mod. Phys. Sci. **1**, 262 (2003).
- [3] A. Sommerfeld, *Thermodynamics and Statistical Mechanics* (Academic Press, New York, 1956).
- [4] G. W. Uhlenbeck and G. V. Ford, *Lectures in Statistical Mechanics* (Amer. Math. Soc., 1963).
- [5] C. Cercignani and R. Penrose, *Ludwig Boltzmann: The Man Who Trusted Atoms* (Oxford University Press, USA, 1998).
- [6] B. Bagchi, *Nonequilibrium Statistical Mechanics: An Introduction with Applications* (CRC Press, Taylor & Francis Group, 2023).
- [7] K. Huang, *Statistical Mechanics* (John Willey & Sons, 1987).
- [8] R. Kubo, M. Toda, and N. Hashitsume, *Statistical Physics II: Nonequilibrium Statistical Mechanics* (Springer-Verlag Berlin Heidelberg GmbH, 1985).
- [9] J. B. Hubbard, S. P. Lund, and M. Halter, *Boltzmann’s H - Function and Diffusion Processes*, J. Phys. Chem. B **117**, 12836 (2013).
- [10] T. Sumikama, S. Saito, and I. Ohmine, *Mechanism of Ion Permeation through a Model Channel: Roles of Energetic and Entropic Contributions*, J. Chem. Phys. **139**, 1 (2013).

- [11] J. Orban and A. Bellemans, *Velocity-Inversion and Irreversibility in a Dilute Gas of Hard Disks*, Phys. Lett. A **24**, 620 (1967).
- [12] E. T. Jaynes, *Violation of Boltzmann's H Theorem in Real Gases*, Phys. Rev. A **4**, 747 (1971).
- [13] F. Bagnoli and R. Rechtman, *Thermodynamic Entropy and Chaos in a Discrete Hydrodynamical System*, Phys. Rev. E **79**, 041115 (2009).
- [14] R. L. Kaufmann and W. R. Paterson, *Boltzmann H Function and Entropy in the Plasma Sheet*, J. Geophys. Res. **114**, A00D04 (2009).
- [15] S. Kumar, S. Acharya, and B. Bagchi, *Sensitivity of Nonequilibrium Relaxation to Interaction Potentials : Timescales of Response from Boltzmann's H Function*, Phys. Rev. E **107**, 24138 (2023).
- [16] J. Kim and T. Keyes, *On the Mechanism of Reorientational and Structural Relaxation in Supercooled Liquids: The Role of Border Dynamics and Cooperativity*, J. Chem. Phys. **121**, 4237 (2004).
- [17] S. Tang and G. T. Evans, *A Critique of Slip and Stick Hydrodynamics for Ellipsoidal Bodies*, Mol. Phys. **80**, 1443 (1993).
- [18] S. Tang, G. T. Evans, C. P. Mason, and M. P. Allen, *Shear Viscosity for Fluids of Hard Ellipsoids: A Kinetic Theory and Molecular Dynamics Study*, J. Chem. Phys. **102**, 3794 (1995).
- [19] R. G. Gordon, *On the Rotational Diffusion of Molecules*, J. Chem. Phys. **44**, 1830 (1966).
- [20] J. G. Gay and B. J. Berne, *Modification of the Overlap Potential to Mimic a Linear Site-Site Potential*, J. Chem. Phys. **74**, 3316 (1981).
- [21] R. Berardi, C. Fava, and C. Zannoni, *A Gay-Berne Potential for Dissimilar Biaxial Particles*, Chem. Phys. Lett. **297**, 8 (1998).

- [22] E. De Miguel, L. F. Rull, M. K. Chalam, K. E. Gubbins, and F. Van Swol, *Location of the Isotropic-Nematic Transition in the Gay-Berne Model*, Mol. Phys. **72**, 593 (1991).
- [23] D. Chakrabarti, P. P. Jose, S. Chakrabarty, and B. Bagchi, *Universal Power Law in the Orientational Relaxation in Thermotropic Liquid Crystals*, Phys. Rev. Lett. **95**, 1 (2005).
- [24] M. P. Allen, D. Frenkel, and J. Talbot, *Molecular Dynamics Simulation Using Hard Particles*, Comput. Phys. Reports **9**, 301 (1989).
- [25] W. C. Swope, H. C. Andersen, P. H. Berens, and K. R. Wilson, *A Computer Simulation Method for the Calculation of Equilibrium Constants for the Formation of Physical Clusters of Molecules: Application to Small Water Clusters*, J. Chem. Phys. **76**, 637 (1982).
- [26] M. P. Allen and D. J. Tildesley, *Computer Simulation of Liquids* (Oxford University Press, USA, 1987).
- [27] B. Bagchi, *Statistical Mechanics for Chemistry and Materials Science* (Francis-Taylor, CRC Press, 2018).
- [28] R. Zwanzig and A. K. Harrison, *Modifications of the Stokes – Einstein Formula*, J. Chem. Phys. **83**, 5861 (1985).
- [29] B. Bagchi, *Molecular Relaxation in Liquids* (Oxford University Press, USA, 2012).
- [30] C. M. Hu and R. Zwanzig, *Rotational Friction Coefficients for Spheroids with the Slipping Boundary Condition*, J. Chem. Phys. **43**, 4354 (1974).
- [31] J. M. Deutch and I. Oppenheim, *Molecular Theory of Brownian Motion for Several Particles*, J. Chem. Phys. **54**, 3547 (1971).
- [32] A. Chandra and B. Bagchi, *A Molecular Theory of Collective Orientational Relaxation in Pure and Binary Dipolar Liquids*, J. Chem. Phys. **91**, 1829 (1989).
- [33] R. Vasanthi, S. Ravichandran, and B. Bagchi, *Needlelike Motion of Prolate Ellipsoids in the Sea of Spheres*, J. Chem. Phys. **114**, 7989 (2001).

- [34] R. Vasanthi, S. Bhattacharyya, and B. Bagchi, *Anisotropic Diffusion of Spheroids in Liquids: Slow Orientational Relaxation of the Oblates*, J. Chem. Phys. **116**, 1092 (2002).